Electron Paramagnetic Resonance Studies of the Coordination Schemes and Site Selectivities for Divalent Metal Ions in Complexes with Pyruvate Kinase†

Jenny L. Buchbinder and George H. Reed*

Institute for Enzyme Research, Graduate School, and Department of Biochemistry, College of Agricultural and Life Sciences, University of Wisconsin—Madison, Madison, Wisconsin 53705

Received August 28, 1989; Revised Manuscript Received October 18, 1989

ABSTRACT: Electron paramagnetic resonance (EPR) spectroscopy has been used to investigate the properties of the binuclear divalent metal center at the active site of pyruvate kinase. The preferred binding sites for different types of divalent cation in complexes of the enzyme with ATP and oxalate were determined in hybrid metal complexes with Mn(II). Superhyperfine coupling between the unpaired electron spin of Mn(II) and the nuclear spin of ^{17}O in isotopically enriched forms of oxalate and ATP was used to determine the position of Mn(II) at the binuclear metal center. When Mn(II) is present in combination with Zn(II), Ni(II), or Co(II), Mn(II) binds predominantly at the site defined by ligands from the protein, oxalate, and the γ-phosphate of ATP. In contrast, EPR data of samples with mixtures of Mn(II)/Ca(II) or Mn(II)/Cd(II) reveal signals of two distinct hybrid–metal complexes. In one species, Mn(II) binds at the oxalate/γ-phosphate site, and Ca(II) or Cd(II) binds at the ATP site. In the other species, the positions of Mn(II) and the second metal ion are reversed. The results indicate that, in enzymic complexes with ATP and oxalate, the relative size of the cation is a major factor controlling site selectivity. Metal ions that have ionic radii smaller than Mn(II) bind preferentially at the site occupied by ATP whereas metal ions that have ionic radii larger than Mn(II) bind preferentially at the site occupied by oxalate. EPR data of one of the hybrid complexes formed by Cd(II) and Mn(II) show that an α,β,γ-tridentate species of $Mn^{II}ATP$ binds to the enzyme. The finding that Mn(II) at either of the divalent cation sites binds to the γ-phosphate group of ATP suggests that the γ-phosphate is linked to both divalent cations in the binuclear divalent metal center.

Pyruvate kinase belongs to a class of enzymes that require multiple equivalents of inorganic cations as cofactors for their catalytic function (Markham, 1986). For pyruvate kinase, a pair of divalent cations and a monovalent cation combine with the anionic substrates at the active site to produce the catalytically competent unit (Gupta et al., 1976; Gupta & Mildvan, 1977; Nowak & Suelter, 1981; Baek & Nowak, 1982). One divalent cation binds directly to the protein in the absence of substrates (site I) (Reuben & Cohn, 1970), and the other divalent cation binds to the enzyme as a complex with the nucleotide substrate (site II) (Gupta et al., 1976; Gupta & Mildvan, 1977). X-ray crystallographic results with the enzyme from cat muscle indicate that a carboxylate from Glu-271 and main-chain carbonyls from Ala-292 and Arg-293 can coordinate to the divalent metal ion at site I (Muirhead et al., 1986).

Substitution of metal ions within multinuclear centers to form metal–hybrid complexes is an effective method for defining individual functions in such centers (Maret & Zeppezauer, 1988). Baek and Nowak (1982) probed the selectivities of the two sites in the binuclear center of pyruvate kinase by kinetic assays involving hybrid mixtures of cations. Synergistic activation of the enzyme by low concentrations of Mn(II) in solutions with high concentrations of Mg(II) indicated that Mn(II) binds selectively at site I (Baek & Nowak, 1982). Lodato and Reed (1987) exploited this selectivity of the two sites for binding of Mn(II) and Mg(II) in EPR[1] spectroscopic studies of enzymic complexes with ATP and an analogue of enolpyruvate, oxalate. The latter investigation showed that Mn(II), at site I, bound to oxalate in a bidentate fashion. Furthermore, the EPR studies identified ATP as a bridging ligand for the two divalent cations, because the γ-phosphate of $Mg^{II}ATP$ contributed an oxygen ligand to Mn(II) at site I. A single water ligand was also identified from the EPR results. The high intracellular concentration of Mg(II) and low intracellular concentrations of other divalent cations make it unlikely that the selectivities of the sites on pyruvate kinase have any physiological significance. This asymmetric, binuclear metal center is, however, a convenient model system for studies of hybrid metal complexes. Mixtures of metal ions with labile ligand exchange properties produce complexes in which thermodynamic stabilities govern the ultimate positions of the metal constituents at the active site.

The preferred isomer of the metal–nucleotide substrate for pyruvate kinase has not been firmly established. The Δ epimer of β,γ-bidentate $Cr^{III}ATP$ functions as a cofactor for the enolization reaction of pyruvate and as a substrate in the phosphorylation of glycolate (Dunaway-Mariano et al., 1979; Dunaway-Mariano & Cleland, 1980). Kinetic studies with the resolved epimers of ADPαS, however, revealed a reversal in epimer selectivity with metal ions of soft and hard Lewis acid character (Jaffe, 1979). Such a result is indicative of metal ion coordination at the α-phosphate group of the nucleotide. Chemical shifts of ^{31}P NMR signals from $Mg^{II}ATP$ in complexes with pyruvate kinase and oxalate had the same values as for $Mg^{II}ATP$ free in solution (Gupta & Mildvan, 1977). Recent experiments with exchange-inert complexes

† This work was supported by Grant GM35752 from the NIH.

* Address correspondence to this author at the Institute for Enzyme Research, University of Wisconsin, 1710 University Ave., Madison, WI 53705.

[1] Abbreviations: EPR, electron paramagnetic resonance; NMR, nuclear magnetic resonance; ADPαS, adenosine 5′-*O*-(1-thiodiphosphate); ATPγS, adenosine 5′-*O*-(3-thiotriphosphate); [α,β-^{17}O]ATP, [$\alpha,\alpha,\alpha\beta,\beta,\beta,\beta\gamma$-$^{17}O$]ATP; [$\alpha,\gamma$-$^{17}O$]ATP, [$\alpha,\alpha,\alpha\beta,\gamma,\gamma,\gamma$-$^{17}O$]ATP; [$\beta,\gamma$-$^{17}O$]-ATP, [$\beta,\beta,\beta\gamma,\gamma,\gamma,\gamma$-$^{17}O$]ATP; [$\alpha,\beta,\gamma$-$^{17}O$]ATP, [$\alpha,\alpha,\alpha\beta,\beta,\beta,\beta\gamma,\gamma,\gamma,\gamma$-$^{17}O$]ATP; HPLC, high-pressure liquid chromatography; P-enolpyruvate, phosphoenolpyruvate.

0006-2960/90/0429-1799$02.50/0

of $Rh^{III}ATP$ indicate that a β,γ-bidentate and an α,β,γ-tridentate complex are both active in the phosphorylation of glycolate catalyzed by the enzyme (Z. Lu, A. L. Shorter, and D. Dunaway-Mariano, personal communication).

In the present study, the well-resolved EPR spectra of Mn(II) in complexes with the enzyme, oxalate, ATP, and several other types of divalent cation are used to investigate the selectivity of the two sites for the cations. EPR data of hybrid metal complexes in which Mn(II) binds at site II are used to determine the coordination scheme of the $Mn^{II}ATP$ substrate.

Experimental Procedures

Materials. Pyruvate kinase was isolated from rabbit skeletal muscle by the method of Tietz and Ochoa (1958). Gel filtration (Sephacryl S-200) was added as a final step in the purification as described previously (Ash et al., 1984). Specific activities of the preparations exceeded 200 IU mg^{-1} in the coupled assay with lactate dehydrogenase at 21 °C. Water enriched to 56 atom % in ^{17}O was obtained from Monsanto. [^{17}O]Oxalate was prepared by acidic exchange as described previously (Ash, 1982; Lodato & Reed, 1987). Samples of ATP enriched in ^{17}O were prepared as described by Leyh et al. (1985). In some samples, synthetic steps were combined to incorporate ^{17}O regiospecifically into more than one phosphate group. Labeled and unlabeled forms of ATP were purified by ion-exchange chromatography on DEAE-Sephadex (A-25). Analytical purity of the ATP was assayed by HPLC with a Whatman Partisil-10 SAX analytical column. Isotopic enrichments in the labeled forms of ATP were determined by ^{31}P NMR (Tsai, 1979). For the [α,β,γ-^{17}O]ATP residual intensities in the ^{31}P NMR signals were quantitated with a calibrated, external standard in a coaxial insert.

EPR Measurements. EPR spectra were recorded at 35 GHz (Q-band) with a Varian E109Q spectrometer. Sample temperature was regulated to ±1 °C with a Varian flow Dewar and temperature controller. The spectrometer was interfaced with an IBM AT microcomputer for data acquisition. Mn(II) binds with a high affinity ($K_d \sim 1$ μM) to the enzyme–oxalate complex (Reed & Morgan, 1974). The concentration of active sites in samples for EPR measurements was in sufficient excess over that of Mn(II) to ensure a virtually stoichiometric binding of Mn(II) in the enzymic complexes. Concentrations of the second divalent cation and of ATP were selected, by titration, to maximize the amplitudes of the new signals that appear upon occupation of both sites for divalent cations. Stock solutions of ^{17}O-enriched substrates were matched in concentration to within ±2% of the corresponding solutions of unlabeled substrates. Identical volumes of these concentration-matched solutions were added to aliquots from a common stock solution containing all of the sample components except for the isotopically labeled substrate. The amplitudes of EPR signals of separate samples, prepared in duplicate, matched to within ±2%. Spectra were simulated by using an analytical expression corrected to third order in the zero-field splitting (D and E) and ^{55}Mn hyperfine coupling (A) terms (Reed & Markham, 1984; Moore & Reed, 1985). A distribution in the zero-field splitting parameters broadens the extremities of the powder patterns, and this line shape effect was modeled in simulations by summing several computed spectra with a Gaussian amplitude and distribution in D (Meirovitch et al., 1974; Reed & Markham, 1984).

EPR Methodology. Experiments reported here use the characteristic EPR absorptions of Mn(II) ($S = {}^5/_2$; $I = {}^5/_2$) in enzymic complexes. The dominant signals in the powder-pattern spectra are from the $M_s\ {}^1/_2 \Leftrightarrow M_s\ {}^{-1}/_2$ fine structure transition. The ^{55}Mn hyperfine sextet in this transition exhibits additional fine structure that originates from second-order terms in the zero-field splitting interaction (Reed & Markham, 1984). The zero-field splitting interaction reflects the electronic symmetry of the coordinated ion, and the powder patterns trace the orientation dependence of this central fine structure transition that results from second and higher order terms in the zero-field splitting interaction. The characteristic time scale for EPR results in a superposition of spectra of each species of Mn(II) in the sample.

Superhyperfine coupling between the unpaired electron spin of Mn(II) and the nuclear spin of a single ^{17}O ($I = {}^5/_2$) ligand atom splits each of the EPR signals into a sextet pattern. This superhyperfine coupling is unresolved in the spectra, because the magnitude of the superhyperfine coupling constant is smaller than the intrinsic line widths of the EPR signals (Reed & Leyh, 1980). The unresolved superhyperfine coupling does, however, appear in the EPR signals as an inhomogeneous broadening. The observed line width is given by (Norris et al., 1971)

$$\Delta H_{obs} = (\Delta H_i^2 + \Delta H_{SHF}^2)^{1/2} \quad (1)$$

where ΔH_{obs} and ΔH_i are the observed and intrinsic line widths and ΔH_{SHF} is the width of the ^{17}O superhyperfine manifold (i.e., ~5 times the magnitude of the ^{17}O superhyperfine coupling constant). This inhomogeneous broadening can be observed in the EPR signals when ΔH_{SHF} is comparable to ΔH_i (Reed & Leyh, 1980).

Enrichments of the labeled ligands in ^{17}O is <56%, and the spectra that are observed experimentally are superpositions of spectra of species in which Mn(II) binds to the nonmagnetic isotopes of oxygen (i.e., ^{16}O and ^{18}O) and of species in which Mn(II) binds to ^{17}O. The statistical weights of the species are determined by the isotopic enrichment in the ligand and by the number of coordination sites occupied by the ligand [see Reed & Leyh (1980) and Lodato and Reed (1987)]. The fraction, F_n, of the sample that has exclusively nonmagnetic isotopes of oxygen ligands is given by

$$F_n = [f(^{16}O) + f(^{18}O)]^n \quad (2)$$

where $f(^{16}O) + f(^{18}O)$ is the fraction of nonmagnetic isotopes and n is the number of coordination sites for the ligand in question. F_n also corresponds to the fraction of the EPR signals that is unperturbed by coupling to ^{17}O, and this fraction diminishes with increases in ^{17}O enrichment and in n. Furthermore, species with two or more ^{17}O ligands experience a greater extent of broadening due to the greater width of the resulting coupling pattern. Hence, for a given isotopic enrichment, the extent of ^{17}O-induced inhomogeneous broadening is greater in spectra of a multiply labeled, multidentate ligand, or of a ligand with multiple sites in the complex, than of a monodentate ligand that occupies a single site. These principles have been exploited in previous studies to determine the number of coordination sites occupied by H_2O (Reed & Leyh, 1980; Moore & Reed, 1985; Lodato & Reed, 1987; Kofron et al., 1988) and the number of oxygen ligands contributed by oxalate in enzymic complexes with Mn(II) (Lodato & Reed, 1987; Kofron et al., 1988). For a multidentate ligand, such as ATP, multiple labeling in the ligand enhances the experimentally observed broadening provided that all of the labeled positions contribute to the coordination sphere of Mn(II).

Results and Discussion

EPR Data of Complexes Containing Mn(II)/Zn(II), Mn(II)/Ni(II), and Mn(II)/Co(II) Mixtures. Lodato and Reed

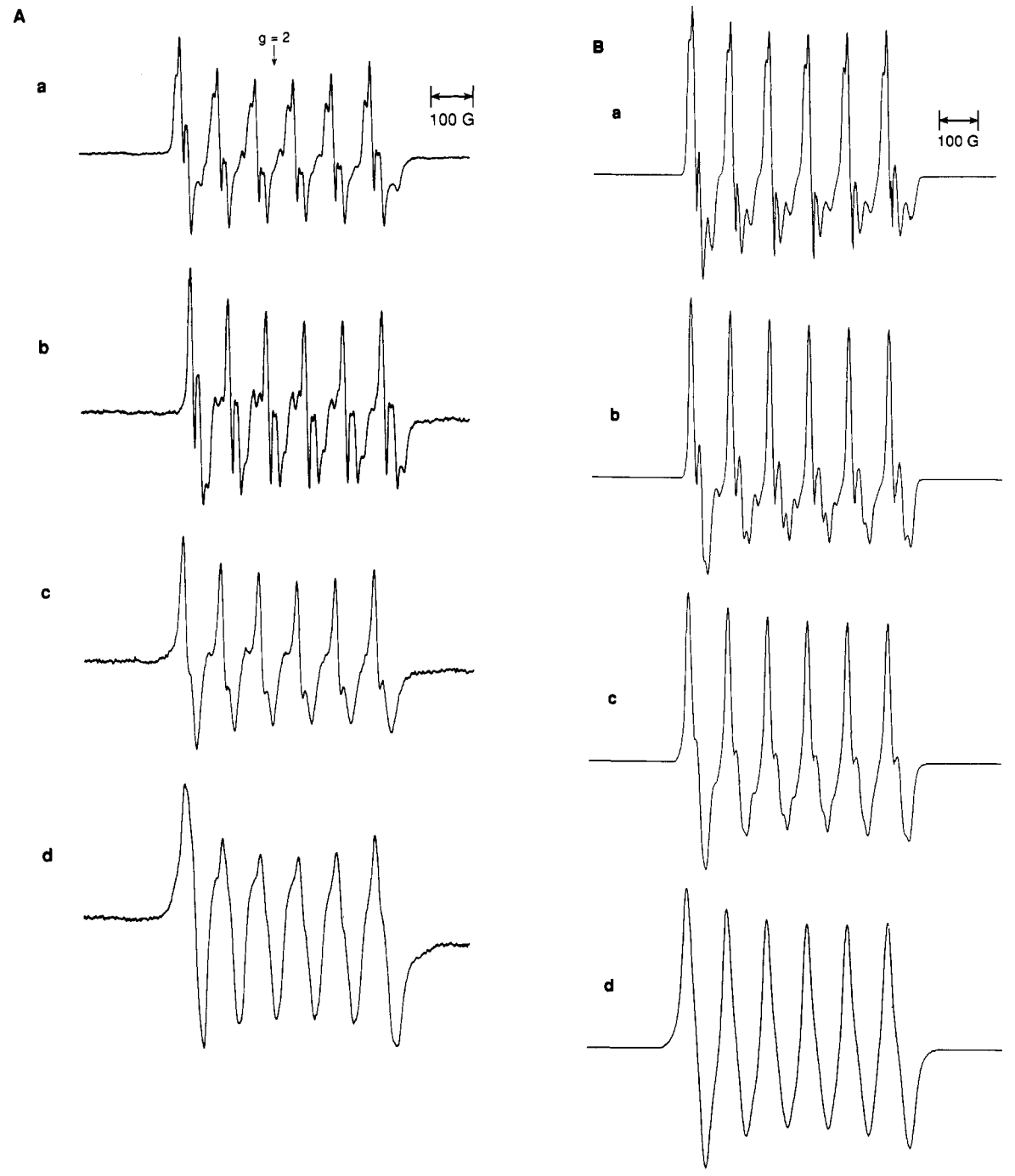

FIGURE 1: Experimental (A) and simulated (B) EPR spectra (Q-band) of Mn(II) in metal–hybrid complexes of pyruvate kinase with Mg(II), Zn(II), Ni(II), or Co(II). (A) (a) The solution contained 50 mM Hepes/$(CH_3)_4NOH$, pH 7.5; 125 mM KCl; 2.6 mM enzyme sites; 6.3 mM oxalate; 5.0 mM ATP; 1.7 mM $MnCl_2$; and 6.3 mM $MgCl_2$. (b) The solution contained 50 mM Hepes/KOH, pH 7.5; 55 mM KCl; 2.3 mM enzyme sites; 5.5 mM oxalate; 2.8 mM ATP; 0.82 mM $MnCl_2$; and 3.6 mM $Zn(OAc)_2$. (c) The solution contained 50 mM Hepes/KOH, pH 7.5; 64 mM KCl; 2.7 mM enzyme sites; 6.4 mM oxalate; 3.9 mM ATP; 0.96 mM $MnCl_2$; and 5.5 mM $NiCl_2$. (d) The solution contained 50 mM Hepes/KOH, pH 7.5; 73 mM KCl; 3.4 mM enzyme sites; 4.8 mM oxalate; 4.5 mM ATP; 1.1 mM $MnCl_2$; and 2.9 mM $CoCl_2$. All of the spectra were obtained at −3 °C. (B) Parameters used in the simulation of the spectra were as follows. (a) Simulation of the spectrum of the complex with Mg(II): D = 300 G, E = 60 G, ΔD = 30 G, $A(^{55}Mn)$ = 90 G, Lorentzian line-width parameter = 2.5 G. (b) Simulation of the spectrum of the complex with Zn(II): D = 270 G, E = 40 G, ΔD = 20 G, $A(^{55}Mn)$ = 90 G, Lorentzian line-width parameter = 4 G. (c) Simulation of the spectrum of the complex with Ni(II): D = 270 G, E = 40 G, ΔD = 20 G, $A(^{55}Mn)$ = 90 G, Lorentzian line-width parameter = 6.5 G. (d) Simulation of the spectrum of the complex with Co(II): D = 270 G, E = 40 G, ΔD = 20 G, $A(^{55}Mn)$ = 90 G, Lorentzian line-width parameter = 12 G. For each of the simulated spectra, 15 spectra with different values of D (half-width of the distribution ΔD) were summed, and their amplitudes were weighted as a Gaussian.

(1987) showed that additions of $MgCl_2$ to solutions of enzyme, $MnCl_2$, oxalate, and ATP resulted in formation of a dominant complex of the form enzyme–oxalate–Mn^{II}–ATP–Mg^{II}. Similarly, titration of a solution of enzyme, $MnCl_2$, oxalate, and ATP with $Zn(OAc)_2$, $NiCl_2$, or $CoCl_2$ produces a new set of EPR signals of the bound Mn(II) (see Figure 1A). The new signals reach maximal amplitudes upon saturation of the complex with the second divalent metal ion. The spectra in Figure 1A do not correspond to those of the bis Mn(II) complex, enzyme–oxalate–Mn^{II}–ATP–Mn^{II} (Lodato & Reed, 1987), and this observation indicates that virtually all of the Mn(II) binds in hybrid metal centers in the samples.

Spectra of the complexes with diamagnetic partners [Zn(II) and Mg(II)] in the hybrid center exhibit relatively narrow

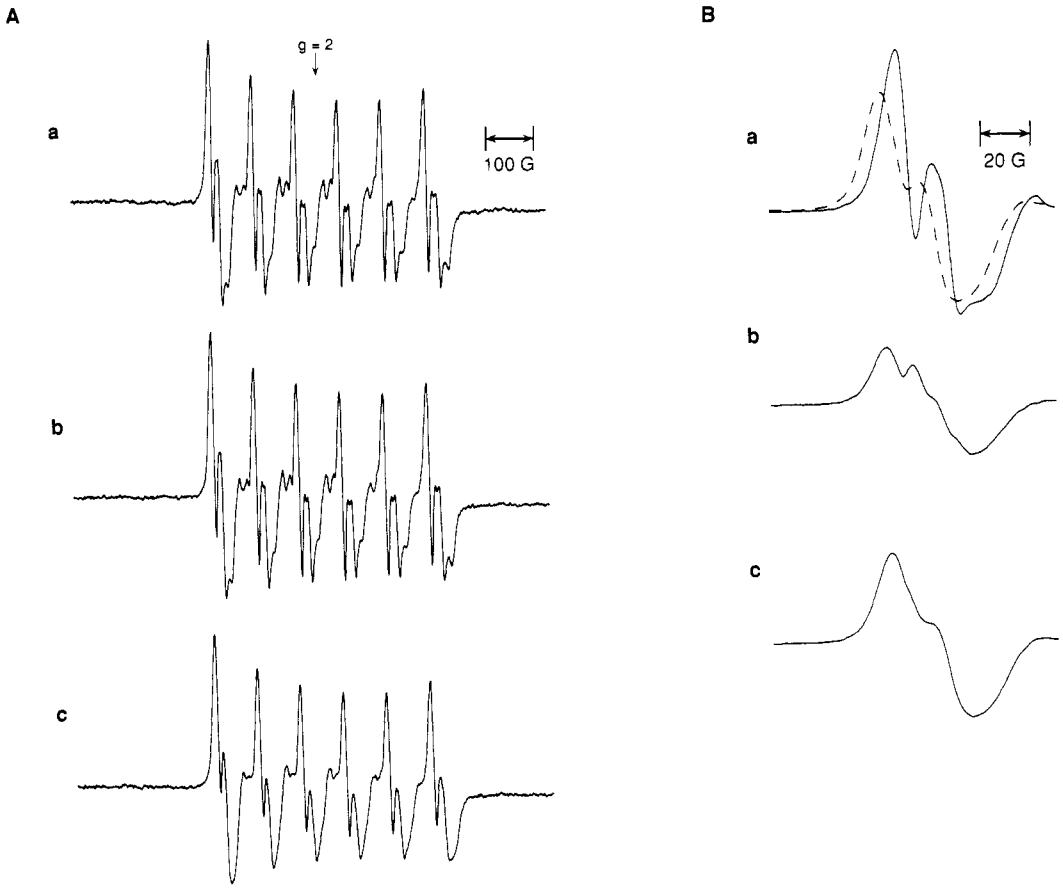

FIGURE 2: EPR spectra (Q-band) of the metal–hybrid complex, enzyme–oxalate–Mn^{II}–ATP–Zn^{II}, with ^{17}O-enriched and unlabeled forms of ATP and oxalate. (A) Solutions contained 50 mM Hepes/KOH, pH 7.5; 55 mM KCl; 2.3 mM enzyme sites; 5.5 mM oxalate; 0.82 mM $MnCl_2$; 3.6 mM $Zn(OAc)_2$; and 2.8 mM ATP or labeled ATP. The ^{17}O enrichment in the labeled forms of ATP was 41 ± 4%. Spectra of samples with (a) unlabeled ATP, with (b) [α-^{17}O]ATP, and with (c) [γ-^{17}O]ATP are shown. Spectra were obtained at −3 °C. (B) Solutions contained 50 mM Hepes/KOH, pH 7.5; 67 mM KCl; 2.8 mM enzyme sites; 1.0 mM $MnCl_2$; 4.4 mM $Zn(OAc)_2$; 4.1 mM ATP; and 6.7 mM oxalate or labeled oxalate. Spectra were obtained at −2 °C. In (a), expansions of the lowest field ^{55}Mn hyperfine line are shown with a solid line for the sample with unlabeled oxalate and with a dashed line for the sample with ^{17}O-enriched oxalate. Spectra in (a) are offset on the abscissa. Curves b and c are difference spectra obtained by subtracting fractions (see eq 2) of the spectrum of the sample with unlabeled oxalate from the spectrum of the sample with ^{17}O-enriched oxalate. For the difference spectrum shown in (b), $F_n = 0.5$, corresponding to a monodentate coordination scheme for oxalate. The trough in (b), which occurs at the field position of the peak in the spectrum of the sample of unlabeled oxalate, is anomalous and indicates that F_n is less than the value corresponding to the monodentate model. For the difference spectrum shown in (c), $F_n = 0.25$, corresponding to a bidentate coordination scheme for oxalate. The absence of anomalous features in this difference spectrum indicates that the bidentate scheme is appropriate for this complex.

signals that permit an appraisal[2] of the zero-field splitting parameters of Mn(II) in the two complexes through spectral simulations (see Figure 1B). The line shapes in experimental spectra of both complexes indicate that there is a finite distribution of zero-field splitting parameters throughout the samples. This distribution was modeled in simulations by a Gaussian distribution in D. The slight difference in zero-field splitting parameters of Mn(II) in the hybrid complexes with Zn(II) and with Mg(II) likely originates from subtle differences in the position or effective charge of the γ-phosphate ligand in the two complexes.

Signals in the spectra of the hybrid complexes with the two paramagnetic ions, Ni(II) and Co(II), are broader than spectra of the complexes with the diamagnetic companion ions. One anticipates that the unpaired electron spins of Ni(II) or Co(II) might exert some influence on the unpaired electrons of the nearby Mn(II), even though the electron spin relaxation times for Ni(II) and Co(II) are short at this high temperature. The spectrum of the hybrid complex with Mn(II) and Ni(II) was modeled with the zero-field splitting parameters used for simulation of the spectrum with Zn(II) by increasing the homogeneous line width. Similarly, the spectrum of the hybrid complex with Mn(II) and Co(II) was modeled with this same set of zero-field splitting parameters by using a slightly greater homogeneous line width. Electron spin–electron spin coupling (scalar and/or anisotropic) is a likely source of the increased line widths in the signals of the hybrid complexes with Ni(II) and with Co(II). Parameters used in the simulations are collected in Table I.

Spectra obtained from samples that contained ^{17}O-enriched forms of oxalate and of ATP were used to confirm the site of Mn(II) binding in the complexes. EPR signals of Mn(II) in samples with mixtures of Mn(II)/Zn(II), Mn(II)/Co(II), or Mn(II)/Ni(II), exhibit inhomogeneous broadening from [^{17}O]oxalate. Signals in the spectra of mixtures of Mn(II) with Zn(II) or Ni(II) are sufficiently narrow to exhibit inhomogeneous broadening from ^{17}O in the γ-phosphate of ATP. Moreover, spectra of samples with [α-^{17}O]ATP or [β-^{17}O]ATP match those of unlabeled ATP. Data of complexes containing the mixture of Mn(II) and Zn(II) are shown in Figure 2. The EPR data show that, in mixtures of Mn(II) with Ni(II), Zn(II), or Co(II), Mn(II) binds selectively at site I where it

[2] The spectrum of the hybrid complex with Mg(II) shows improved resolution with increases in the concentration of K^+ from 80 to 125 mM. The improved resolution in the experimental spectrum permits a better estimate of the zero-field splitting parameters than those reported previously (Lodato & Reed, 1987).

Table I: Parameters Used for Simulated Spectra in Figure 1B[a]

complex	D (G)	E (G)	ΔW[b] (G)	ΔD[c] (G)
E-oxalate-Mn-ATP-Mg	300	60	2.5	30
E-oxalate-Mn-ATP-Zn	270	40	4	20
E-oxalate-Mn-ATP-Ni	270	40	6.5	20
E-oxalate-Mn-ATP-Co	270	40	12	20

[a] For each of the simulated spectra, 15 spectra with different values of D, half-width of distribution ΔD, were summed and their amplitudes were weighted in a Gaussian fashion. A ^{55}Mn hyperfine coupling const. of 90 G was used in all simulations. [b] ΔW is the Lorentzian line width. [c] ΔD is the half-width of the Gaussian distribution in the axial zero-field splitting parameter.

receives two oxygen ligands from oxalate and an oxygen ligand from the γ-phosphate of ATP. The companion metal ions bind to site II as complexes with ATP.

EPR Data of Complexes Containing Mn(II)/Cd(II) Mixtures. The EPR spectrum obtained of samples with mixtures of Mn(II) and Cd(II) (see Figure 3A) contains more signals than can be assigned to second-order fine structure from a single species[3] of complexed Mn(II). The signals divide into two groups. An interval equal to the ^{55}Mn hyperfine coupling constant separates the six major signals in each group. One set of signals (marked O) occur at the same field positions where signals of Mn(II) at site I appear in spectra of samples with other types of divalent cation. [The two prominent features of the O signals in each hyperfine transition coincide with analogous features in the spectra of hybrid complexes with Zn(II) or with Mg(II).] The remaining group of signals (marked N) are components of a more anisotropic powder pattern. The O signals obscure the upfield features of the N patterns in all but the highest field ^{55}Mn hyperfine transition. This overlap between components of the two subspectra distorts the appearance of the individual powder patterns.

The origins of the N and O signals can be determined from measurements with ^{17}O-enriched forms of oxalate and ATP. [^{17}O]Oxalate broadens[4] one set of signals (O signals) in the spectrum (see Figure 3B), and these signals are therefore assigned to the spectrum of Mn(II) at site I in a hybrid complex of the form enzyme-oxalate-Mn^{II}-ATP-Cd^{II}. The N signals have greater intrinsic line widths than the O signals, and the extent of inhomogeneous broadening from ATPs labeled regiospecifically at a single phosphate group is measurable but modest. The multiply labeled forms of ATP were therefore used to enhance the effects of ^{17}O on these signals. Results from one set of experiments are shown in Figure 4. All of the N and O signals are broadened when the γ-phosphate is one of the ^{17}O-labeled positions. This observation shows that the γ-phosphate contributes a ligand to each form of complexed Mn(II) represented in the spectrum. In contrast, only the N signals are broadened by [α,β-^{17}O]ATP. The broadening of the N signals in samples with [α,β-^{17}O]ATP permits an unambiguous assignment of this group of signals to the spectrum of Mn(II) at site II in a hybrid complex of the form enzyme-oxalate-Cd^{II}-ATP-Mn^{II}. The data of Figure 4 also define the structure of the Mn^{II}ATP chelate bound at site II. ^{17}O in the α position of ATP makes an

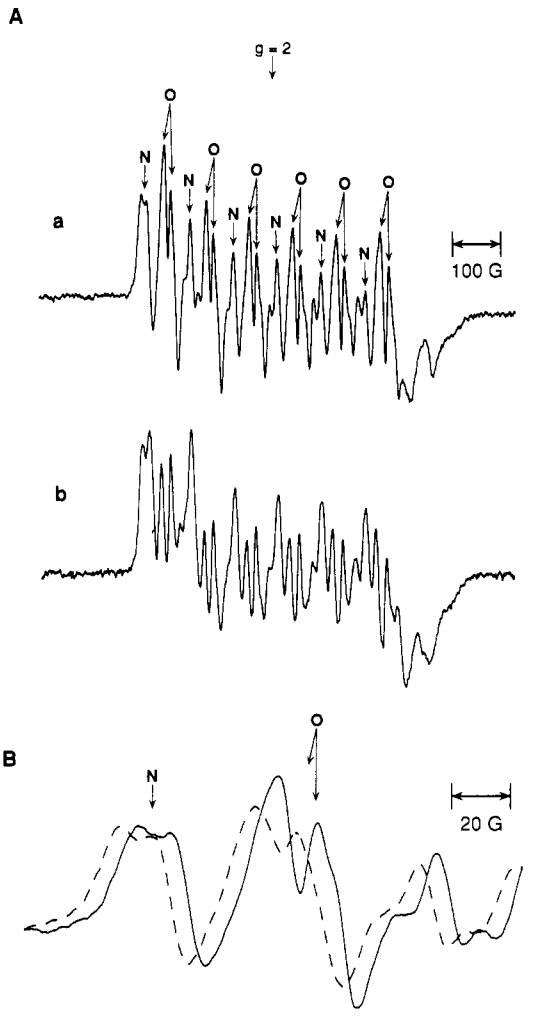

FIGURE 3: EPR spectra of samples containing mixtures of Mn(II) and Cd(II) or Mn(II) and Ca(II). (A) (a) Q-band EPR spectrum of a sample containing Mn(II) and Cd(II). The solution contained 50 mM Hepes/KOH, pH 7.5; 145 mM KCl; 3.4 mM enzyme sites; 2.0 mM $MnCl_2$; 3.9 mM $CdCl_2$; 4.8 mM ATP; and 9.1 mM oxalate. The signals marked N and O belong to different species of complexed Mn(II). (b) Q-band EPR spectrum of Mn(II) in hybrid complexes of pyruvate kinase with Ca(II). The solution contained 50 mM Hepes/KOH, pH 7.5; 64 mM KCl; 2.8 mM enzyme sites; 6.4 mM oxalate; 2.6 mM ATP; 0.96 mM $MnCl_2$; and 6.0 mM $CaCl_2$. All spectra were obtained with samples at −2 °C. (B) Expansions of the lowest field ^{55}Mn^{II} hyperfine components in the spectra of samples of the Mn(II)/Cd(II) hybrid mixture with labeled (dashed line) and unlabeled (solid line) oxalate. The spectra are offset on the abscissa.

important contribution to broadening of the N signals, because the extent of inhomogeneous broadening in spectra of samples with [α,β-^{17}O]ATP and with [α,γ-^{17}O]ATP is significantly greater than those observed in spectra of samples with the singly labeled forms, [β-^{17}O]ATP or [γ-^{17}O]ATP (not shown). Also [α,β,γ-^{17}O]ATP produces the greatest extent of broadening in the N signals. These data show that an α,β,γ-tridentate chelate of Mn^{II}ATP binds at site II.

The relative amounts of the two complexes formed in the samples containing mixtures of Mn(II) and Cd(II) are difficult to assess quantitatively because the signals are only partly resolved. The properties of powder patterns, however, permit a qualitative assessment of the relative concentrations of the two complexes. The subspectrum represented by the N signals has the greater zero-field splitting anisotropy. In the first-derivative observation of powder patterns, increases in anisotropy reduce the amplitudes of the signals. The relative amplitudes of the O and N signals, together with their respective line widths and anisotropies, indicate that the complex

[3] The ADP/ATP ratio of <0.01 in samples that were quenched by addition of $CHCl_3$ and assayed for nucleotide composition by HPLC showed that the two sets of signals did not arise from a mixture of substrate and product (i.e., ATP-oxalate and ADP-oxalyl phosphate) complexes. None of the signals correspond to signals of potential non-enzymic complexes of Mn(II), e.g., Mn^{II}-oxalate or Mn^{II}ATP.

[4] Overlap of the patterns of the O and N subspectra results in a slight perturbation in the amplitudes of some of the N signals in samples with labeled oxalate.

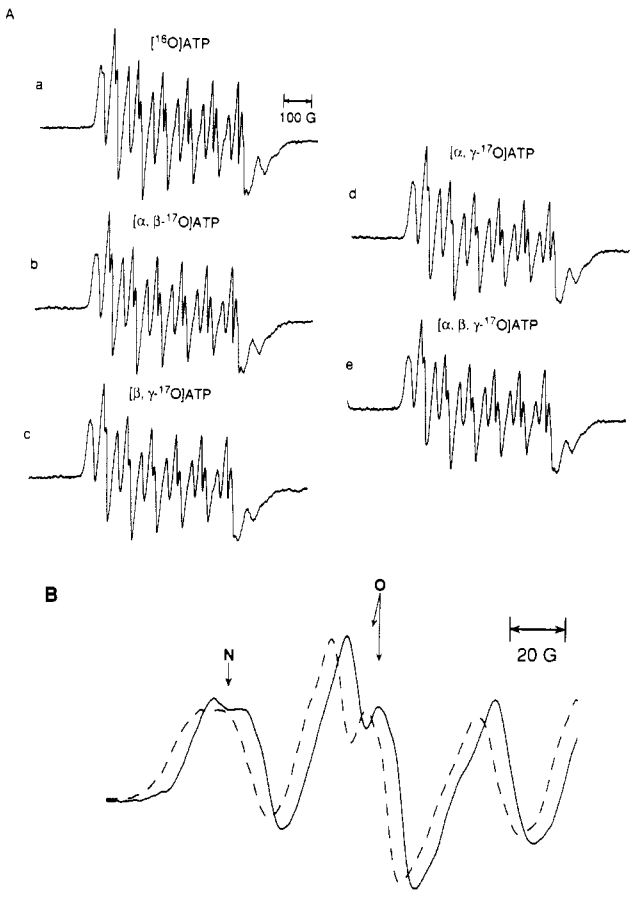

FIGURE 4: Effect of ^{17}O in ATP on EPR spectra (Q-band) of Mn(II) in metal–hybrid complexes of pyruvate kinase with Cd(II). Solutions contained 50 mM Hepes/KOH, pH 7.5; 69 mM KCl; 3.0 mM enzyme sites; 1.0 mM $MnCl_2$; 3.8 mM $CdCl_2$; 6.9 mM oxalate; and 2.6 mM ATP or labeled ATP. Spectra were obtained at −2 °C. (A) Spectra of samples with (a) unlabeled ATP, (b) [α,β-^{17}O]ATP (26% at α and 27% at β), (c) [β,γ-^{17}O]ATP (44% at β and 29% at γ), (d) [α,γ-^{17}O]ATP (26% at α and 29% at γ), and (e) [α,β,γ-^{17}O]ATP (26% at α, 27% at β, and 27% at γ). ^{17}O enrichments at the labeled phosphate positions in the nucleotides are noted in parentheses. (B) Expansions of the lowest field $^{55}Mn^{II}$ hyperfine components in the spectra. The spectrum of the sample with unlabeled ATP is shown with a solid line, and the spectrum of the sample with [α,β-^{17}O]ATP is shown with a dashed line. Spectra are offset on the abscissa.

in which Mn(II) binds at site II is more abundant.

EPR Data of Complexes Containing Mn(II)/Ca(II) Mixtures. A gradual precipitation of Ca^{II}–oxalate in samples containing enzyme, oxalate, ATP, $MnCl_2$, and $CaCl_2$ leads to a time dependence in the EPR spectra that complicates detailed assignments of signals in the spectrum. The pattern of signals in spectra of samples with mixtures of Mn(II) and Ca(II) (see Figure 3A) is similar to that found for the mixtures of Mn(II) and Cd(II). The influences of ^{17}O in oxalate and in ATP (not shown) on these signals indicate qualitatively that the signals have origins that are analogous to those found for mixtures of Mn(II) and Cd(II) [i.e., two hybrid complexes form which differ in the positions of Mn(II) and Ca(II)].

Effects of Monovalent Cations on Spectra of Mn(II)/Cd(II) Complexes. The type of monovalent cation present in the solution influences the EPR spectrum of Mn(II) in hybrid complexes with all of the divalent cations that were examined. Representative data of samples containing mixtures of Mn(II) and Cd(II) are shown in Figure 5. Spectra obtained of samples containing the nonactivating monovalent cation $(CH_3)_4N^+$ (Kayne, 1971) are poorly resolved, and it is not clear that a species in which Mn(II) binds at site II makes a contribution to this spectrum. In contrast, spectra of samples

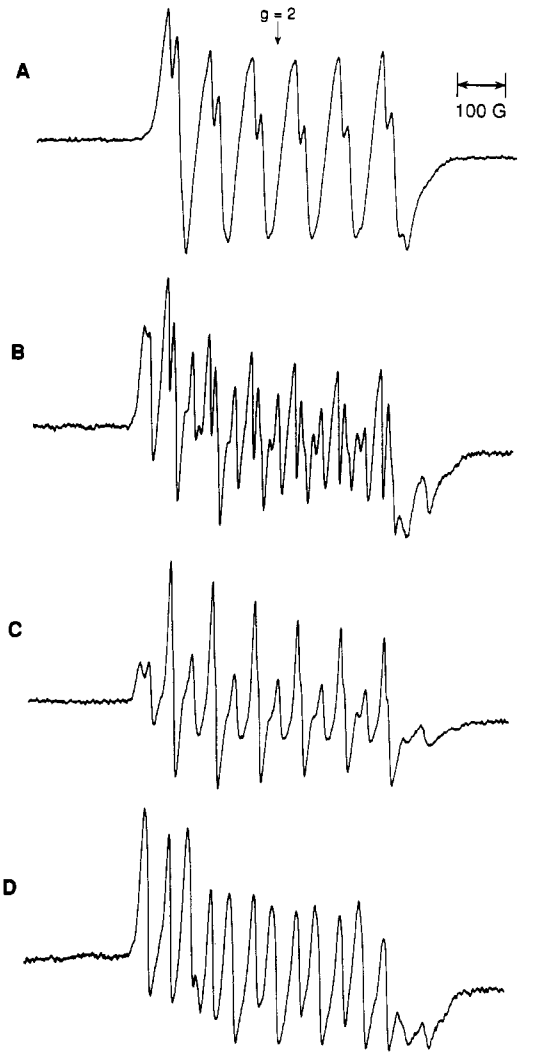

FIGURE 5: Effect of monovalent cations on EPR spectra (Q-band) of Mn(II) in metal–hybrid complexes of pyruvate kinase with Cd(II). (A) Sample with $(CH_3)_4N^+$. Solution contained 50 mM Hepes/$(CH_3)_4NOH$, pH 7.5; 40 mM tetramethylammonium acetate; 4.0 mM enzyme sites; 9.1 mM tetramethylammonium oxalate; 4.8 mM Tris–ATP; 2.0 mM $MnCl_2$; and 3.8 mM $Cd(OAc)_2$. (B) Sample with K^+. Solutions contained 50 mM Hepes/KOH, pH 7.5; 145 mM KCl; 3.4 mM enzyme sites; 9.1 mM Tris–oxalate; 4.8 mM Tris–ATP; 2.0 mM $MnCl_2$; and 3.9 mM $CdCl_2$. (C) Sample with NH_4^+. Solution contained 50 mM Hepes/$(CH_3)_4NOH$, pH 7.5; 50 mM NH_4Cl; 2.9 mM enzyme sites; 9.1 mM tetramethylammonium oxalate; 5.3 mM ATP; 2.0 mM $MnCl_2$; and 4.2 mM $CdCl_2$. (D) Sample with Tl^+. Solution contained 50 mM Hepes/$(CH_3)_4NOH$, pH 7.5; 10 mM $TlNO_3$; 2.8 mM enzyme sites; 9.1 mM tetramethylammonium oxalate; 4.5 mM ATP; 1.8 mM $MnCl_2$; and 3.8 mM $Cd(OAc)_2$. All of the spectra were obtained at −2 °C.

containing the activating cations NH_4^+ or Tl^+ resemble spectra of samples containing K^+; i.e., there are two sets of signals indicative of two types of hybrid complexes. Spectra of the samples containing NH_4^+ or Tl^+ do, however, differ, in detail, from those of samples with K^+. For example, the amplitudes of signals from Mn(II) at site I are greater in the samples containing NH_4^+. The doublet character of the signals from Mn(II) at site I is also absent in spectra of samples containing either NH_4^+ or Tl^+. The latter observation indicates that the type of monovalent cation influences the zero-field splitting interaction for Mn(II) at site I. The assignments of signals in spectra of samples with Tl^+ were confirmed by measurements with the ^{17}O-enriched ligands (data not shown).

Kinetic Studies with Hybrid Mixtures. Baek and Nowak (1982) reported a synergistic activation of the physiological reaction with mixtures of Mn(II) and Co(II). The observed

Table II: Positions of Metal Ions in Complexes of Pyruvate Kinase, ATP, and Oxalate with Mn^{2+} Present as the Companion Species; Dissociation Constants[a] of the Respective Free Metal Ligand Complexes; and Ionic Radii[b] of Metal Ions

metal ion	site[c] in enzymic complex with Mn(II)	pK_d^{ATP}	$pK_d^{oxalate}$	r (Å)
Mg^{2+}	site II[d]	3.77	2.55	0.65
Co^{2+}	site II	4.62	4.7	0.74
Ni^{2+}	site II	4.61	5.3	0.69
Zn^{2+}	site II	4.26	5.0	0.74
Ca^{2+}	sites I and II	3.77	3	0.94
Cd^{2+}	sites I and II	4.7	4	0.92
Mn^{2+}		4.75	3.8	0.80

[a] Dissociation constants of metal–ATP and of metal–oxalate complexes were obtained from compilations by Phillips (1966) and by Clifford (1961), respectively. [b] Ionic radii as given by Pauling, compiled by Cotton and Wilkinson (1972). [c] Site I has ligands from oxalate, γ-phosphate of ATP, water, and the protein. Site II has ligands from the α-, β-, and γ-phosphates of ATP. [d] Lodato and Reed (1987).

synergism indicated that Mn(II) bound at site I and Co(II) bound at site II. Results from the EPR experiments indicate that Ni(II) and Zn(II) as well as Co(II) bind preferentially at site II in the presence of Mn(II), ATP, and oxalate. Synergistic activation with mixtures of Mn(II) and Zn(II) or Mn(II) and Ni(II) would be expected if site I retained its selectivity for Mn(II) in the presence of the physiological substrates and if either Zn^{II}ADP or Ni^{II}ADP were more effective substrates than Mn^{II}ADP. Steady-state kinetics experiments, similar to those of Baek and Nowak (1982), were conducted to determine whether synergistic activation would occur with these metal ions. As reported by Baek and Nowak (1982), Zn(II) or Ni(II) alone supports a low level of activity. Gradual replacement of Zn(II) or Ni(II) by Mn(II), while the total concentration of divalent cations is held constant at 1 or 2 mM, results in monotonic increases in steady-state velocity (not shown). Assays having low concentrations of Mn(II), 1–50 μM, give no indication of synergism between Mn(II) and either Zn(II) or Ni(II).

Conclusions. The selectivities observed for the binuclear divalent metal center in pyruvate kinase are summarized in Table II, and a schematic representation of the center is shown in Figure 6. The stabilities of the metal–oxalate and metal–ATP complexes free in solution do not correlate with the selectivities in the enzymic complexes. In fact, the observed selectivities are contrary to what one would predict for mixtures of Mn(II) with Co(II), Zn(II), and Ni(II) based on the relative stabilities of the respective ATP and oxalate complexes in solution. The pattern of site selectivities does, however, relate to the ionic radii of the cations. All of the cations that have ionic radii smaller than Mn(II) bind at site II when Mn(II) is their partner in the center. The two cations that have ionic radii larger than Mn(II), namely, Cd(II) and Ca(II), distribute between sites I and II to give a mixture of two hybrid complexes with Mn(II).

The kinetic method (Foster et al., 1967; Baek & Nowak, 1982) reveals information about site selectivity only when there is synergism in activation by two species of divalent cation. The combination of ATP and oxalate might impart different selectivities on the sites than the combination of ADP and P-enolpyruvate. However, for two cases where synergistic activation was found kinetically—namely, hybrid mixtures of Mn(II) with either Mg(II) or Co(II)—the site selectivities of the enzyme–oxalate–ATP species agree with the selectivities inferred from kinetic behavior (Baek & Nowak, 1982).

The α,β,γ-tridentate coordination scheme found for Mn^{II}ATP in the complex enzyme–oxalate–Cd^{II}–ATP–Mn^{II} agrees with the interpretation of an α-phosphate–metal ion

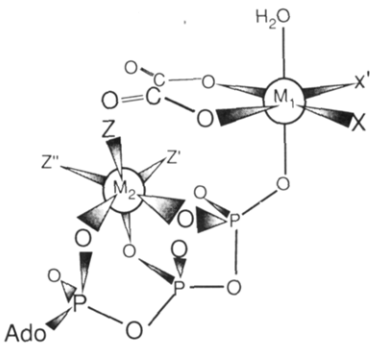

FIGURE 6: Schematic drawing showing oxalate, ATP, and two divalent cations bound at the active site of pyruvate kinase. M_1 is the divalent cation at site I, and M_2 is the divalent cation at site II. Four oxygen ligands for M_1 have been identified by EPR experiments with ^{17}O labeling. Ligands X and X′ are contributed from the protein. The α,β,γ-tridentate coordination scheme for M_2 was determined for Mn(II) at this site in one of the hybrid complexes formed in the presence of Cd(II). The stereochemical configurations of the α,β- and β,γ-chelate rings depicted in the figure are in accordance with the work of Jaffe (1979) and of Dunaway-Mariano and Cleland (1979), respectively. Ligands Z, Z′, and Z″ have not been identified in the present studies. These ligands are likely water molecules, given the facile binding of the aquo–Cr^{III}ATP species at this site (Dunaway-Mariano & Cleland, 1979).

coordination that was suggested by the results from kinetic studies conducted with epimers of ADPαS (Jaffe, 1979). The tridentate coordination scheme for the enzyme-bound Mn^{II}ATP complex also agrees with recent activity patterns found for isomers of Rh^{III}ATP in the enzyme-catalyzed phosphorylation of glycolate (Z. Lu, A. L. Shorter, and D. Dunaway-Mariano, personal communication).

The combination of enzyme, ATP, and oxalate is a genuine product complex, because synthetic oxalyl phosphate phosphorylates ADP in a reaction catalyzed by pyruvate kinase (Kofron & Reed, 1988). In enzymic complexes with ATP and oxalate, the γ-phosphate of ATP contributes a ligand to Mn(II) when this cation binds either at site I or at site II. Although the present results do not establish, unequivocally, that the respective companion metal ions bind to the γ-phosphate concurrently, an attractive structure for the divalent metal center is one in which both divalent cations bind to the γ-phosphate group (see Figure 6). This bridging ligand arrangement constrains the two divalent cations to within ~4.5–5.8 Å center to center on the basis of measurements from molecular models. A previous estimate (Gupta, 1977) of a 7.5-Å separation of Cr(III) and Mn(II) in a complex with enzyme, oxalate, and Cr^{III}ATP was based on observation of an ~20% decrease in the amplitudes of EPR signals of enyzme-bound Mn(II) at X-band in the presence of the Cr(III)–nucleotide complex. More recent EPR measurements at Q-band (Lodato, 1986) show a much larger decrease (~80%) in the amplitudes of EPR signals of Mn(II) in the enzymic complex with oxalate upon binding of Cr^{III}ATP. The latter experiments indicate a Cr(III)-to-Mn(II) distance of ~5 Å. Coordination of two of the pendant oxygen atoms from the γ-phosphate to electrophilic metal centers prepares P_γ for nucleophilic attack by an oxygen. This nucleophilic oxygen is, itself, a ligand for metal I in the center. The two divalent cations are also situated such that their coordination spheres can serve as templates for this in-line (Blattler & Knowles, 1979) phospho-transfer step.

The type of monovalent cation present influences the EPR spectra of Mn(II) in the hybrid complexes with ATP and oxalate. These spectroscopic observations suggest that an activating monovalent cation is required to promote a proper

coordination of Mn(II) at either of the two divalent cation sites. Although the present EPR data do not offer information on the position or number of monovalent cations that bind at the active site, a structure in which the carboxylate group of the substrate bridges one monovalent cation and metal I (Lodato & Reed, 1987) is consistent with available experimental data (Reuben & Kayne, 1971; Hutton et al., 1977; Raushel & Villafranca, 1980; Ash et al., 1978; Lord & Reed, 1987).

ACKNOWLEDGMENTS

We thank Dr. Debra Dunaway-Mariano for communication of results prior to publication and David Latwesen for assistance with spectral simulations. ^{31}P NMR spectra were obtained at the National Magnetic Resonance Facility at Madison (NIH Grant RR02301).

REFERENCES

Ash, D. E. (1982) Ph.D. Thesis, University of Pennsylvania.
Ash, D. E., Kayne, F. J., & Reed, G. H. (1978) *Arch. Biochem. Biophys. 190*, 571–577.
Ash, D. E., Goodhart, P. J., & Reed, G. H. (1984) *Arch. Biochem. Biophys.* 228, 31–40.
Baek, Y. H., & Nowak, T. (1982) *Arch. Biochem. Biophys. 217*, 491–497.
Blattler, W. A., & Knowles, J. R. (1979) *Biochemistry 18*, 3927–3933.
Clifford, A. F. (1961) *Inorganic Chemistry of Qualitative Analysis*, pp 451–452, Prentice Hall, NJ.
Cotton, F. A., & Wilkinson, G. (1972) *Advanced Inorganic Chemistry*, 2nd ed., p 52, Wiley Interscience, New York.
Dunaway-Mariano, D., & Cleland, W. W. (1980) *Biochemistry 19*, 1506–1515.
Dunaway-Mariano, D., Benovic, J. L., Cleland, W. W., Gupta, R. K., & Mildvan, A. S. (1979) *Biochemistry 18*, 4347–4354.
Foster, D. O., Lardy, H. A., Ray, P. D., & Johnson, J. B. (1967) *Biochemistry 6*, 2120–2128.
Gupta, R. K. (1977) *J. Biol. Chem. 252*, 5183–5185.
Gupta, R. K., & Mildvan, A. S. (1977) *J. Biol. Chem. 252*, 5967–5976.
Gupta, R. K., Oesterling, R. M., & Mildvan, A. S. (1976) *Biochemistry 15*, 2881–2887.
Hutton, W. C., Stephens, E. M., & Grisham, C. M. (1977) *Arch. Biochem. Biophys. 184*, 166–171.
Jaffe, E. K. (1979) Ph.D. Thesis, University of Pennsylvania.
Kayne, F. J. (1971) *Arch. Biochem. Biophys. 143*, 232–239.
Kofron, J. L., & Reed, G. H. (1988) *FASEB J. 2*, A587.
Kofron, J. L., Ash, D. E., & Reed, G. H. (1988) *Biochemistry 27*, 4781–4787.
Leyh, T. S. Goodhart, P. J., Nguyen, A. C., Kenyon, G. L., & Reed, G. H. (1985) *Biochemistry 24*, 308–316.
Lodato, D. T. (1986) Ph.D. Thesis, University of Pennsylvania.
Lodato, D. T., & Reed, G. H. (1987) *Biochemistry 26*, 2243–2250.
Lord, K. A., & Reed, G. H. (1987) *Inorg. Chem. 26*, 1464–1466.
Markham, G. D. (1986) in *Manganese in Metabolism and Enzyme Function* (Schramm, V. L., & Wedler, F. C., Eds.) pp 379–403, Academic Press, Orlando, FL.
Maret, W., & Zeppezauer, M. (1988) *Methods Enzymol. 158*, 79–94.
Meirovitch, E., Luz, Z., & Kalb, A. J. (1974) *J. Am. Chem. Soc. 96*, 7538–7542.
Moore, J. M., & Reed, G. H. (1985) *Biochemistry 24*, 5328–5333.
Muirhead, H., Clayden, D. A., Barford, D., Lorimer, C. G., Fothergill-Gillmore, L. A., Schiltz, E., & Schmitt, W. (1986) *EMBO J. 5*, 475–481.
Norris, J. R., Uphaus, R. A., Crespi, H. L., & Katz, J. J. (1971) *Proc. Natl. Acad. Sci. U.S.A. 68*, 625–628.
Nowak, T., & Suelter, C. H. (1981) *Mol. Cell. Biochem. 35*, 65–75.
Phillips, R. (1966) *Chem. Rev. 66*, 501–527.
Raushel, F. M., & Villafranca, J. J. (1980) *Biochemistry 19*, 5481–5485.
Reed, G. H., & Morgan, S. D. (1974) *Biochemistry 13*, 3537–3541.
Reed, G. H., & Leyh, T. S. (1980) *Biochemistry 19*, 5472–5480.
Reed, G. H., & Markham, G. D. (1984) *Biol. Magn. Reson. 6*, 73–142.
Reuben, J., & Cohn, M. (1970) *J. Biol. Chem. 245*, 6539–6546.
Reuben, J., & Kayne, F. J. (1971) *J. Biol. Chem. 246*, 6227–6234.
Teitz, A., & Ochoa, S. (1958) *Arch. Biochem. Biophys. 78*, 477–493.
Tsai, M.-D. (1979) *Biochemistry 18*, 1468–1472.